AMERICAN SOCIETY FOR MICROBIOLOGY | Journal of Bacteriology®

RESEARCH ARTICLE

Dissolved Inorganic Carbon-Accumulating Complexes from Autotrophic Bacteria from Extreme Environments

Sarah Schmid,[a] Dale Chaput,[b] Mya Breitbart,[c] Rebecca Hines,[a] Samantha Williams,[a] Hunter K. Gossett,[a] Sheila D. Parsi,[a] Rebecca Peterson,[a] Robert A. Whittaker,[a] Angela Tarver,[d] Kathleen M. Scott[a]

[a]Department of Integrative Biology, University of South Florida, Tampa, Florida, USA
[b]Proteomics Core Facility, University of South Florida, Tampa, Florida, USA
[c]College of Marine Science, University of South Florida, Tampa, Florida, USA
[d]U.S. Department of Energy Joint Genome Institute, Berkeley, California, USA

ABSTRACT In nature, concentrations of dissolved inorganic carbon (DIC; CO_2 + HCO_3^- + CO_3^{2-}) can be low, and autotrophic organisms adapt with a variety of mechanisms to elevate intracellular DIC concentrations to enhance CO_2 fixation. Such mechanisms have been well studied in *Cyanobacteria*, but much remains to be learned about their activity in other phyla. Novel multisubunit membrane-spanning complexes capable of elevating intracellular DIC were recently described in three species of bacteria. Homologs of these complexes are distributed among 17 phyla in *Bacteria* and *Archaea* and are predicted to consist of one, two, or three subunits. To determine whether DIC accumulation is a shared feature of these diverse complexes, seven of them, representative of organisms from four phyla, from a variety of habitats, and with three different subunit configurations, were chosen for study. A high-CO_2-requiring, carbonic anhydrase-deficient (Δ*yadF* Δ*cynT*) strain of *Escherichia coli* Lemo21(DE3), which could be rescued via elevated intracellular DIC concentrations, was created for heterologous expression and characterization of the complexes. Expression of all seven complexes rescued the ability of *E. coli* Lemo21(DE3) Δ*yadF* Δ*cynT* to grow under low-CO_2 conditions, and six of the seven generated measurably elevated intracellular DIC concentrations when their expression was induced. For complexes consisting of two or three subunits, all subunits were necessary for DIC accumulation. Isotopic disequilibrium experiments clarified that CO_2 was the substrate for these complexes. In addition, the presence of an ionophore prevented the accumulation of intracellular DIC, suggesting that these complexes may couple proton potential to DIC accumulation.

IMPORTANCE To facilitate the synthesis of biomass from CO_2, autotrophic organisms use a variety of mechanisms to increase intracellular DIC concentrations. A novel type of multisubunit complex has recently been described, which has been shown to generate measurably elevated intracellular DIC concentrations in three species of bacteria, raising the question of whether these complexes share this capability across the 17 phyla of *Bacteria* and *Archaea* where they are found. This study shows that DIC accumulation is a trait shared by complexes with various subunit structures, from organisms with diverse physiologies and taxonomies, suggesting that this trait is universal among them. Successful expression in *E. coli* suggests the possibility of their expression in engineered organisms synthesizing compounds of industrial importance from CO_2.

KEYWORDS autotroph, carbon dioxide, carbon dioxide-concentrating mechanism, carbon fixation, dissolved inorganic carbon

Chemolithoautotrophs link redox and carbon cycles by fixing dissolved inorganic carbon (DIC; CO_2 + HCO_3^- + CO_3^{2-}) while using reduced inorganic compounds as electron donors. These microorganisms thrive in environments where compounds

Citation Schmid S, Chaput D, Breitbart M, Hines R, Williams S, Gossett HK, Parsi SD, Peterson R, Whittaker RA, Tarver A, Scott KM. 2021. Dissolved inorganic carbon-accumulating complexes from autotrophic bacteria from extreme environments. J Bacteriol 203:e00377-21. https://doi.org/10.1128/JB.00377-21.

Editor Julie A. Maupin-Furlow, University of Florida

Address correspondence to Kathleen M. Scott, kmscott@usf.edu.

Received 16 July 2021
Accepted 14 September 2021
Accepted manuscript posted online 20 September 2021
Published 5 November 2021

such as H_2S or H_2 are present, including deep-sea hydrothermal vents (1), terrestrial hot springs (2), marine sediment (3), and acid mine drainage (4). In these habitats, redox substrate and DIC availability may vary spatially and temporally, as it does at hydrothermal vents (5, 6).

Many autotrophic microorganisms adapt to low availability of DIC in their environment with a variety of mechanisms to elevate intracellular DIC concentrations, in order to facilitate CO_2 fixation (7–9). To date, there are five known mechanisms for elevating intracellular DIC concentrations. These include three evolutionarily independent types of HCO_3^- transporters: ATP-hydrolyzing ABC transporter BCT1 (10), and sodium-bicarbonate symporters BicA (11) and SbtA (12). Some *Cyanobacteria* also use modified NADH dehydrogenase complexes to convert intracellular CO_2 into HCO_3^- to prevent diffusion of DIC out of the cell (13).

The most recently described means of elevating intracellular DIC concentrations is by a family of multisubunit complexes, whose mechanism of action has yet to be determined. These DIC-accumulating complexes (DACs) were first described in hydrothermal vent chemolithoautotroph *Hydrogenovibrio crunogenus* (8, 14), *Staphylococcus aureus* (15), and *Halothiobacillus neapolitanus* (16). In these organisms, DACs consist of two subunits; one subunit is a membrane-spanning protein (M subunit; Pfam00361), another is a cytoplasmic protein belonging to a family of unknown function (C subunit; Pfam10070), and both subunits are required for DACs to function (8, 16). Disrupting the genes encoding these complexes impairs growth under low-DIC conditions, and intracellular DIC concentrations are measurably elevated when DACs are expressed either in their native hosts or in *Escherichia coli* (8, 14–16). Heterologous expression of DACs from *Vibrio cholerae* and *Bacillus anthracis* in a high-CO_2-requiring strain of *E. coli* restores its ability to grow under low-DIC conditions, suggesting that these two DACs also elevate intracellular DIC concentrations (16). The protonophore carbonyl cyanide *m*-chlorophenyl hydrazone (CCCP) inhibits DIC accumulation by DACs from *H. crunogenus*, *S. aureus*, and *H. neapolitanus* (8, 14, 16), indicating that activity may be coupled to proton motive force. These studies suggest that DACs may all function similarly to elevate intracellular DIC concentrations.

However, the evidence for shared function is compromised by the limited diversity of DACs that have been studied, which include five DACs representing mesophiles and neutrophiles from two phyla, all with two-subunit structure. This sample does not represent DACs adequately; genes encoding DACs are present in organisms from 16 phyla of *Bacteria* (*Acidobacteria*, *Actinobacteria*, *Aquificae*, *Bacteroidetes*, *Chlamydiae*, *Chloroflexi*, *Deinococcus*, *Firmicutes*, *Gemmatimonadetes*, *Nitrospinae*, *Nitrospirae*, *Planctomycetes*, *Proteobacteria*, *Rhodothermaeota*, *Spirochaetes*, *Verrucomicrobia*) and one phylum of *Archaea* (*Euryarchaeota*) (Integrated Microbial Genomes and Microbiomes database [https://img.jgi.doe.gov], accessed 15 June 2021), which thrive at a broad range of temperatures, osmolarities, and pH values. DACs also are predicted to have a diversity of subunit structures beyond the two-subunit DACs that have already been studied. In some organisms, e.g., *Acidimicrobium ferrooxidans*, C and M proteins are fused into a single protein with domains belonging to Pfam10070 and Pfam00361. In other organisms, a third tiny subunit (T subunit) is encoded by a small gene that is found between those encoding the M and C subunits (Fig. 1). Some organisms carry genes for more than one DAC (9); for example, *H. neapolitanus* has a two-subunit DAC (characterized in reference 16), and a three-subunit DAC whose activity has not been characterized. Given this breadth in taxonomy and structure, assuming shared function seems unwise.

The substrate for DACs (CO_2 or HCO_3^-) is also unclear. In *S. aureus*, this complex was predicted to be a Na^+:HCO_3^- cotransporter (15), while in *H. neapolitanus*, the response of DIC accumulation to pH provided evidence that this complex uses CO_2 as a substrate (16).

Clarifying the function and substrate of DACs is relevant to understanding their ubiquity in 17 phyla of microorganisms with every imaginable lifestyle, from autotrophic extremophile to deadly pathogen. DACs have been suggested to facilitate CO_2

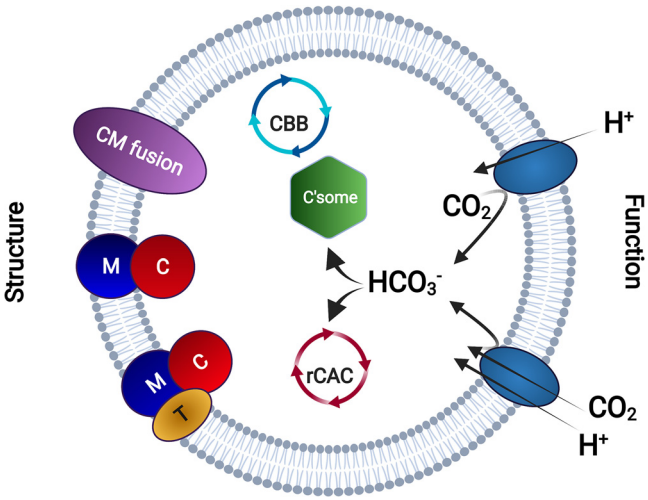

FIG 1 Models for structure and function of DACs. Possible configurations of 1-, 2-, and 3-subunit forms of DACs are depicted on the left. Both T and M subunits are predicted by TMHMM (32) to have multiple membrane-spanning alpha helices and are accordingly shown spanning the membrane. On the right, two possible models for DAC function are shown, one in which DACs couple proton translocation to the conversion of intracellular CO_2 to HCO_3^- and one in which DACs carry out symport of CO_2 and protons and this CO_2 is converted to HCO_3^- during or upon translocation to the cytoplasm. In autotrophic cells, this HCO_3^- is consumed by the Calvin-Benson-Bassham cycle (CBB) via carboxysomes (c'some) or the reductive citric acid cycle (rCAC). This figure was created with BioRender.com.

fixation by autotrophic bacteria in the many, sometimes extreme, habitats where they form the base of the food web (8, 9, 14). They have also been suggested to facilitate pathogenesis under conditions where boosting anapleurotic CO_2 fixation could provide an advantage (15, 16).

The objectives of this study were to confirm whether (i) DACs from a variety of organisms can indeed raise concentrations of intracellular DIC, (ii) all subunits (including T, when present) are necessary for activity, and (iii) DACs use the same substrate (CO_2 or HCO_3^-) and are similarly sensitive to disruption of proton motive force. Seven complexes were selected, with amino acid sequence identities ranging from 31 to 73%, to span DAC diversity (Table 1): four phyla are represented, as is a full range of pH preferences for growth (acidophilic to alkaliphilic) and subunit compositions predicted from genome data (1 subunit, 2 subunit, and 3 subunit).

RESULTS

Construction of plasmids and an *E. coli* host strain for expressing DACs. Genes encoding DACs from seven species of bacteria (Table 1) were synthesized and cloned into plasmids with weak (pENTR; native), moderate (pBAD202; $araB_p$), and strong (pET28; T7) promoters. A strain of *E. coli* was constructed for expressing DACs, in which genes encoding carbonic anhydrase (*yadF* and *cynT*) were knocked out [*E. coli* Lemo21 (DE3) Δ*yadF* Δ*cynT*]. This strain requires a headspace enriched in CO_2 for growth (see Fig. S1 in the supplemental material). Its ability to grow under ambient air was restored via heterologous expression of genes encoding DACs (see below).

LC-MS/MS confirmation of expression of DACs. Liquid chromatography-tandem mass spectrometry (LC-MS/MS) of cell proteins confirmed the expression of genes encoding C subunits from DACs (Table 2). Peptides derived from C subunits were more abundant when cells were cultivated in the presence of inducer than when cells were cultivated in the presence of repressor, except for *Thermocrinis ruber*, where the number of peptides increased in the presence of repressor, as did the intensity of the signal. It should be noted that the intensity of signal from C subunits overall was low for this particular construct. M-subunit peptide abundance and signal intensities followed the same general pattern, though peptides derived from M subunits were less abundant and their

TABLE 1 Traits of the organisms hosting the seven DACs that are the subjects of this study

Organism	Phylum, class, order, family	Environment	Growth pH	Temp range	Autotrophic pathway[a]	DAC subunit composition
Acidimicrobium ferrooxidans	*Actinobacteria*, *Acidimicrobiia*, *Acidimicrobiales*, *Acidimicrobiaceae*	Hot spring (33)	Acidic	Thermophile	CBB	MC[b]
Acidithiobacillus ferrooxidans	*Proteobacteria*, *Acidithiobacillia*, *Acidithiobacillales*, *Acidithiobacillaceae*	Acid mine drainage (34)	Acidic	Mesophile	CBB	M, C
Acidithiobacillus thiooxidans	*Proteobacteria*, *Acidithiobacillia*, *Acidithiobacillales*, *Acidithiobacillaceae*	Clay formation (35)	Acidic	Mesophile	CBB	M, T, C
Hydrogenovibrio crunogenus	*Proteobacteria*, *Gammaproteobacteria*, *Thiotrichales*, *Piscirickettsiaceae*	Hydrothermal vent (36)	Neutral, alkaline	Mesophile	CBB	M, C
Halothiobacillus neapolitanus	*Proteobacteria*, *Gammaproteobacteria*, *Chromatiales*, *Halothiobacillaceae*	Dissolved concrete (37)	Neutral	Mesophile	CBB	M, T, C
Sulfurovum sp. strain AR	*Campylobacterota*, unclassified, unclassified, unclassified	Marine sediments (38)	Neutral, alkaline	Mesophile	rCAC	M, T, C
Thermocrinis ruber	*Aquificae*, *Aquificae*, *Aquificales*, *Aquificaceae*	Hot spring (39)	Neutral, alkaline	Hyper-thermophile	rCAC	M, TC[c]

[a]CBB, Calvin-Benson-Bassham cycle; rCAC, reductive citric acid cycle.
[b]Complex exists as a single fused protein.
[c]T and C subunits are fused into a single protein.

TABLE 2 Subunits of DACs detected by LC-MS/MS

Species	Subunit	IMG gene ID[a]	No. of peptides[b,c]				Signal intensity[c,d]			
			I	R	No T	M only	I	R	No T	M only
At. ferrooxidans	C	642789231	33	27	—	0	3.3E+10	9.0E+09	—	—
	M	642789232	4	0	—	2	7.3E+08	0	—	—
Am. ferrooxidans	CM	644951280	27	0	—	—	6.8E+09	0	—	—
At. thiooxidans	C	2838919134	59	16	44	0	4.6E+10	8.1E+08	1.1E+10	0
	M	2838919132	8	0	4	6	9.3E+09	0	3.9E+08	2.0E+09
	T	2838919133	5	2	0	0	2.7E+09	1.8E+07	0	0
H. crunogenus	C	637785574	56	30	—	0	8.6E+11	4.7E+10	—	0
	M	637785573	8	0	—	6	1.2E+10	0	—	2.0E+09
H. neapolitanus	C	646383292	51	18	43	0	1.5E+11	2.0E+09	8.7E+10	0
	M	646383294	8	1	7	10	8.8E+09	8.0E+06	9.2E+08	3.8E+09
	T	646383293	3	0	0	0	1.1E+09	0	0	0
Sulfurovum sp. AR	C	2620607600	45	35	50	0	2.1E+10	8.0E+09	3.8E+10	0
	M	2620607602	0	0	0	0	0	0	0	0
	T	2620607601	1	1	0	0	9.8E+07	8.0E+07	0	0
T. ruber	C	2512918850	26	36	—	0	5.1E+09	7.8E+09	—	0
	M	2512918849	0	0	—	0	0	0	—	0

[a]Joint Genome Institute Integrative Microbial Genomes and Microbiomes gene object ID number (https://img.jgi.doe.gov/).
[b]Total number of peptides corresponding to each subunit. I, induced; R, repressed; no T, construct in which the gene encoding the T subunit was omitted, grown in the presence of inducer; M, construct in which the gene encoding the C subunit (and also the T subunit, as applicable) was omitted.
[c]—, not applicable; 0, not detected.
[d]Intensity values for each protein were calculated by summing the extracted chromatograms for each peptide identified.

signal intensities were low in general; they were not detected in constructs expressing DAC from *T. ruber* or *Sulfurovum* sp. strain AR. This may be due to the difficulty of solubilizing and digesting membrane proteins, and it was observed previously for the DAC from *H. crunogenus* (14).

Growth of *E. coli* constructs expressing DACs. *E. coli* Lemo21(DE3) Δ*yadF* Δ*cynT* carrying plasmids encoding complete DACs were able to grow under low-CO_2 conditions. When driven by native promoters, expression of DACs facilitated growth on solid media under low-CO_2 conditions, despite likely weak expression in *E. coli* from promoters originating from organisms from different phyla (Fig. S1). When *E. coli* Lemo21 (DE3) Δ*yadF* Δ*cynT* with DAC gene expression controlled by either the T7 promoter or $araB_p$ were cultivated in liquid media, response to repressors and inducers varied among the DACs, potentially due to toxic effects of the higher levels of expression. Four of the DACs were expressed successfully from pBAD202 vectors; the presence of arabinose (inducer) stimulated growth (e.g., shorter lag times, more high growth rates, or higher yield) (Fig. 2), while glucose (repressor) inhibited it. For the remaining three DACs, expression in pET vectors was successful: growth was stimulated by the presence of IPTG (isopropyl-β-D-thiogalactopyranoside; inducer) and inhibited by rhamnose (repressor, via induction of T7 lysozyme [17]). Constructs without the gene encoding either the C or T subunit were unable to grow under low-CO_2 conditions, regardless of the inclusion of an inducer (Fig. 3). These constructs were able to grow only when provided with a high-CO_2 environment.

Intracellular DIC concentrations in *E. coli* expressing DACs. To prepare for measuring intracellular DIC concentrations, *E. coli* Lemo21(DE3) Δ*yadF* Δ*cynT* carrying plasmids encoding complete or incomplete DACs was cultivated under a 5% CO_2 headspace before harvesting. The concentration of intracellular DIC in *E. coli* Lemo21(DE3) Δ*yadF* Δ*cynT* expressing DACs was measured via silicone oil centrifugation, which assayed [^{14}C]DIC accumulation in the cells (8). Six of the seven DACs were able to generate measurably elevated intracellular DIC concentrations when cells were cultivated in the presence of inducer to stimulate expression of DAC genes (Fig. 4). Cells grown in

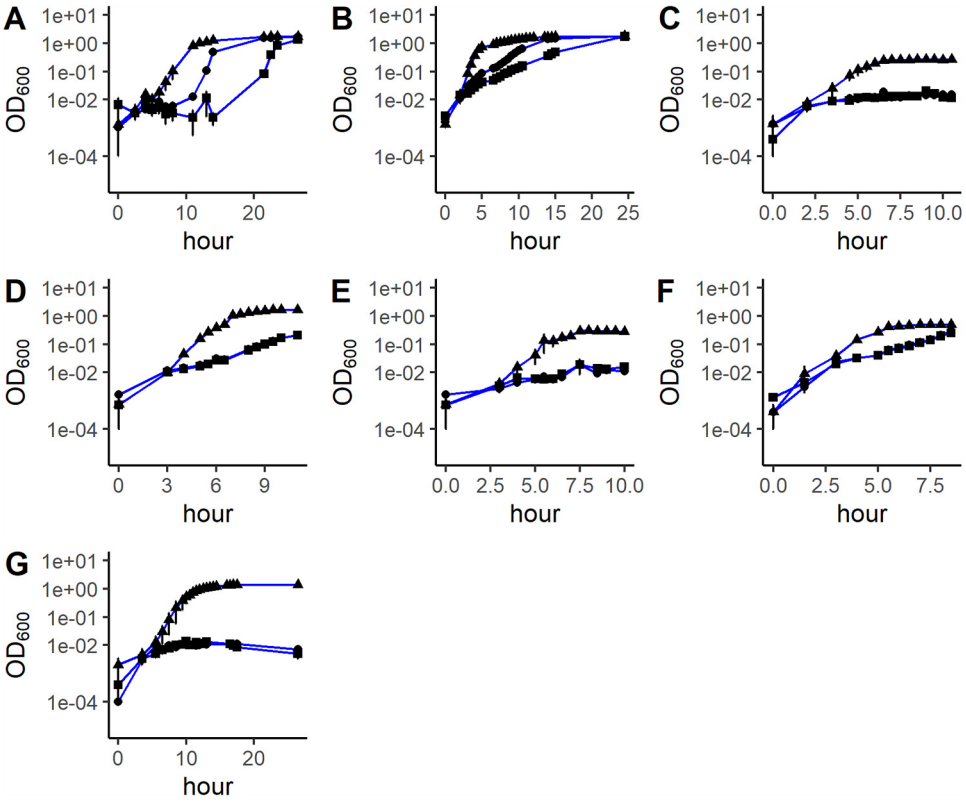

FIG 2 Growth curves of *E. coli* expressing complete DACs under low-CO_2 conditions. Each plot represents growth of a construct expressing a DAC from a different species: (A) *Am. ferrooxidans* DAC genes in pET28; (B) *At. ferrooxidans* in pET28; (C) *At. thiooxidans* in pBAD202; (D) *H. crunogenus* in pBAD202; (E) *H. neapolitanus* in pBAD202; (F) *Sulfurovum* sp. strain AR in pBAD202; (G) *T. ruber* in pET28. Circles, no inducer or repressor; triangles, inducer (IPTG for pET28 constructs; arabinose for pBAD202 constructs); squares, repressor (rhamnose for pET28 constructs; glucose for pBAD202).

the presence of repressor, as well as those expressing incomplete complexes, were unable to generate elevated intracellular DIC concentrations.

A two-way analysis of variance (ANOVA) was undertaken to determine factors resulting in statistically distinguishable concentrations of intracellular DIC. For each DAC, intracellular DIC concentrations measured for each of the following four samples were compared: complete DAC with inducer, complete DAC with repressor, incomplete DAC with inducer, and incomplete DAC with repressor. Only two samples (complete DAC with inducer and complete DAC with repressor) were compared for constructs from *Am. ferrooxidans* because this DAC consists of a single subunit (Table 3). Bonferroni *post hoc* tests were used to determine which factors resulted in statistically distinguishable differences in intracellular DIC concentrations. When constructs with the complete DACs were grown with inducer, intracellular DIC was higher than that of all constructs grown with repressor except the *T. ruber* construct ($P = 1.0$). Constructs that contained only the M subunit or were missing the T subunit did not have appreciably elevated intracellular DIC concentrations.

DAC substrate: HCO_3^- or CO_2. Three DACs, representing one-subunit (*Am. ferrooxidans*), two-subunit (*H. crunogenus*), and three-subunit forms (*Sulfurovum* sp. strain AR), were chosen to clarify the form of DIC used as a substrate, by providing CO_2 or HCO_3^- out of chemical equilibrium. When *E. coli* expressing these DACs was provided with CO_2, intracellular DIC concentrations were higher than when it was provided with HCO_3^- (Fig. 5). A two-way ANOVA was used to compare DIC species (CO_2 and HCO_3^-) and media (with inducer or with repressor). As described above, Bonferroni *post hoc* tests were used to determine which variables resulted in statistically distinguishable

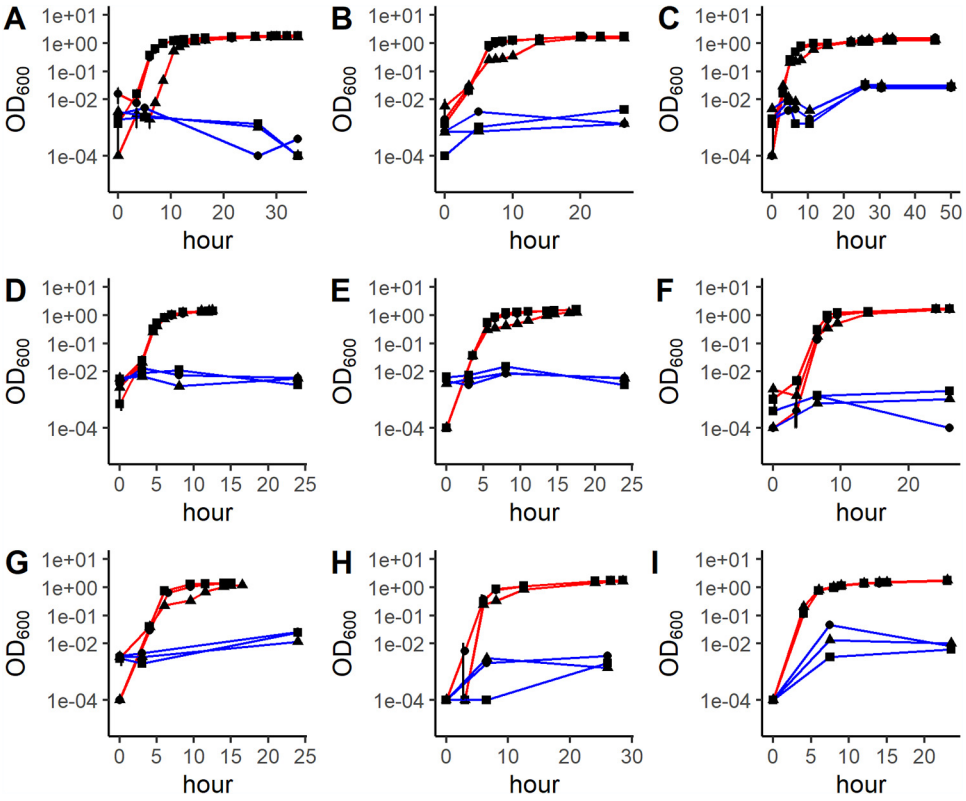

FIG 3 Growth curves of *E. coli* expressing DACs with missing subunits under high-CO_2 (red) and low-CO_2 (blue) conditions. Each plot represents growth of *E. coli* expressing a DAC from a different species: (A) *At. ferrooxidans* DAC genes in pET28, M subunit only; (B) *At. thiooxidans* DAC genes in pBAD202, M subunit only; (C) *At. thiooxidans* DAC genes in pBAD202, C and M subunits only (missing T subunit gene); (D) *H. crunogenus* DAC genes in pBAD202, M subunit only; (E) *H. neapolitanus* DAC genes in pBAD202, M subunit only; (F) *H. neapolitanus* DAC genes in pBAD, C and M subunits only (missing T subunit gene); (G) *Sulfurovum* sp. strain AR DAC genes in pBAD202, M subunit only; (H) *Sulfurovum* sp. strain AR DAC genes in pBAD202, C and M subunits only (missing T subunit); (I) *T. ruber* DA genes in in pET28, M subunit only. Circles, no inducer or repressor; triangles, inducer (IPTG for pET28 constructs; arabinose for pBAD202 constructs); squares, repressor (rhamnose for pET28 constructs; glucose for pBAD202).

differences in intracellular DIC concentrations. For all three DACs, intracellular DIC concentrations were significantly higher when their expression was induced and the cells were provided with CO_2 instead of HCO_3^- (Table 4). *E. coli* carrying genes encoding DACs from *H. crunogenus* and *Sulfurovum* sp. strain AR did not have a significant difference in intracellular DIC concentration when provided with HCO_3^- in the presence of inducer or repressor. When grown in the presence of inducer, they did have measurable accumulation of DIC when HCO_3^- was provided, though this amount was far smaller than when CO_2 was provided (Fig. 5). This may be due to small amounts of CO_2 present in incubations in which HCO_3^- was provided as the dominant form of DIC.

Use of proton potential for DIC accumulation. For *E. coli* expressing the three DACs selected for further study, the addition of protonophore CCCP diminished intracellular DIC concentrations (Fig. 6). The difference between intracellular DIC concentrations in *E. coli* provided with CCCP (dissolved in dimethyl sulfoxide [DMSO]) and those supplied with DMSO only (solvent control) was significant (*t* test $\alpha = 0.05$) when DACs from *Am. ferrooxidans* ($P < 0.001$) and *H. crunogenus* ($P < 0.001$) were expressed but not for the DAC from *Sulfurovum* sp. strain AR ($P = 0.07$).

The effect of CCCP on the intracellular DIC concentration was likely due to its effect on the proton motive force. Cells incubated with CCCP had lower intracellular pH values (Table 5). Furthermore, cells treated with CCCP also had lower intracellular ATP concentrations than those in the control medium (Table 5), as expected if ATP synthase was inhibited by a diminishment in proton motive force. Interestingly, DMSO itself also affected

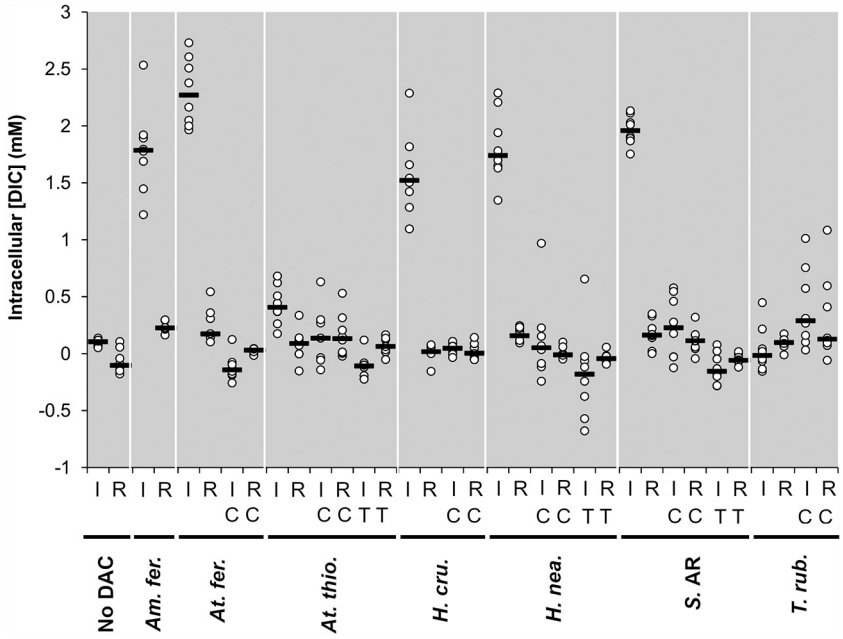

FIG 4 Intracellular DIC concentrations measured in *E. coli* expressing DACs from seven species (Am. fer., *Acidimicrobium ferrooxidans*; At. fer., *Acidithiobacillus ferrooxidans*; At. thio., *Acidithiobacillus thiooxidans*; H. cru., *Hydrogenovibrio crunogenus*; H. nea., *Halothiobacillus neapolitanus*; S. AR, *Sulfurovum* sp. AR; T. rub., *Thermocrinis ruber*). Results are shown for cells grown under a 5% CO_2 headspace in the presence of inducer (I) or repressor (R). When indicated, cells were missing either cytoplasmic (C) or tiny (T) subunits. Black bars indicate median values (n = 8).

intracellular ATP concentrations compared with control medium (Table 5), though less so than when CCCP was also present. This may explain why intracellular DIC concentrations are lower for solvent control experiments (Fig. 6) than when DMSO was absent (Fig. 6).

Relative abundance of genes encoding DACs and Sbt transporters in metagenomes from alkaline and acidic environments. The presence of DAC genes compared to those encoding Sbt-type HCO_3^- transporters appears to be dependent on the pH of the environment from which the samples were collected. The abundance of DAC relative to that of Sbt increases as pH decreases from very alkaline to acidic (Table 6). The analysis of both clusters of orthologous groups (COGs) and Pfams showed the same trend.

TABLE 3 *P* values from statistical analysis of DIC accumulation by cells expressing DACs

	***P* value for:**			
	ANOVA[a]		**Bonferroni[b]**	
Species	**Induced and repressed: complete vs incomplete**	**Complete and incomplete: induced vs repressed**	**Induced: complete vs incomplete**	**Complete: induced vs repressed**
Am. ferrooxidans	NA	NA	NA	<0.001
At. ferrooxidans	<0.001	<0.001	<0.001 (complete vs no C subunit)	<0.001
At. thiooxidans	<0.001	0.23	0.03 (complete vs no C subunit) <0.001 (complete vs no T subunit)	0.0015
H. crunogenus	<0.001	<0.001	<0.001 (complete vs no C subunit)	<0.001
H. neapolitanus	<0.001	<0.001	<0.001 (complete vs no C subunit) <0.001 (complete vs no T subunit)	<0.001
Sulfurovum sp. strain AR	<0.001	<0.001	<0.001 (complete vs no C subunit) <0.001 (complete vs no T subunit)	<0.001
T. ruber	0.007	0.84	0.09 (complete vs no C subunit)	1

[a]For ANOVA, two factors were included in the model: completeness of the DACs and induction of expression. The first column shows *P* values for including completeness as a factor, and the second column shows *P* values for including induction as a factor.

[b]For Bonferroni *post hoc* tests, concentrations of intracellular DIC for cells growing in the presence of inducer were compared for cells with genes encoding complete DACs versus those with incomplete DACs (e.g., missing a C or T subunit [first column]). Bonferroni tests were also used to compare intracellular DIC pools for cells with genes encoding complete DACs, when organisms were grown in the presence of inducer versus repressor (second column).

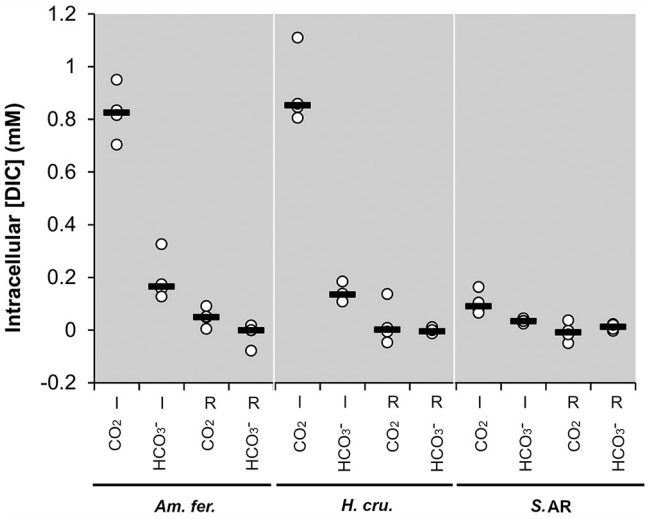

FIG 5 Intracellular DIC concentrations measured for *E. coli* expressing DACs when provided with either CO_2 or HCO_3^- out of chemical equilibrium. *Am. fer.*, *Acidimicrobium ferrooxidans*; *H. cru.*, *Hydrogenovibrio crunogenus*; *S.* AR, *Sulfurovum* sp. strain AR. Results are shown for cells grown in the presence of inducer (I) or repressor (R). Black bars indicate median values ($n = 4$).

DISCUSSION

DACs have been identified in 17 phyla to date, and the results here suggest that they can all facilitate intracellular DIC accumulation from the environment. DACs with all three subunit configurations, gathered from members of the phyla *Actinobacteria*, *Proteobacteria*, *Campylobacterota*, and *Aquificae* inhabiting diverse habitats (e.g., hot springs, acid mine drainage, and marine sediments) with a broad range of pH values (acidic to basic), all share this capability. The juxtaposition of the genes encoding these seven complexes to genes encoding enzymes necessary for autotrophic CO_2 fixation (Fig. 7) suggests that DIC is their substrate when they are expressed in their native organisms. These seven organisms grow autotrophically via the Calvin-Benson-Bassham (CBB) cycle or reductive citric acid cycle (rCAC), indicating that DACs are compatible with a variety of autotrophic metabolisms. Furthermore, DACs are found in heterotrophic organisms as well, suggesting that they contribute to cellular growth in general (15).

Despite their origins in phylogenetically diverse organisms from very different habitats, six of the seven DACs studied here could be successfully expressed in *E. coli*. Unsurprisingly, their "preferred" promoters varied; different promoters resulted in different growth yields (four were higher with $araB_p$, and three were higher with T7). This difference may be due to the effect of overproduction of the expressed proteins, as has been documented in membrane proteins using pET vectors with IPTG as an inducer (17). In order for any of these

TABLE 4 *P* values from statistical analysis of DIC accumulation by cells with genes encoding complete DACs, provided with either CO_2 or HCO_3^-

	ANOVA[a]		Bonferroni[b]		
Organism	HCO_3^- and CO_2: induced vs repressed	Induced and repressed: HCO_3^- vs CO_2	Induced: HCO_3^- vs CO_2	HCO_3^-: induced vs repressed	CO_2: induced vs repressed
Am. ferrooxidans	<0.001	<0.001	<0.001	0.009	<0.001
H. crunogenus	<0.001	<0.001	<0.001	0.17	<0.001
Sulfurovum sp. strain AR	<0.001	0.121	0.04	1	0.001

[a]For ANOVA, two factors were included in the model: form of DIC provided and induction of expression. The first column consists of the *P* values for including induction as a factor, and the second column consists of the *P* values for including form of DIC as a factor.

[b]For Bonferroni *post hoc* tests, concentrations of intracellular DIC for cells growing in the presence of inducer were compared for cells provided with HCO_3^- versus CO_2 (first column). Bonferroni tests were also used to compare the intracellular DIC concentrations of cells grown in the presence of inducer versus repressor for cells provided with HCO_3^- (second column) or CO_2 (third column).

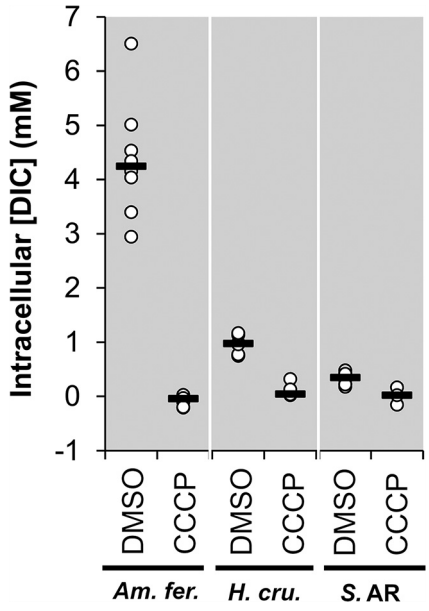

FIG 6 Intracellular DIC concentrations measured in *E. coli* expressing DACs when incubated in the presence of either DMSO (solvent control) or CCCP plus DMSO. *Am. fer.*, *Acidimicrobium ferrooxidans*; *H. cru.*, *Hydrogenovibrio crunogenus*; *S.* AR, *Sulfurovum* sp. strain AR. Black bars indicate median values ($n = 8$).

DACs to rescue *E. coli* Lemo21(DE3) Δ*yadF* Δ*cynT*, it is necessary for the DAC to be able to generate a high enough intracellular DIC concentration to support metabolism. However, accumulating excessive intracellular DIC might affect intracellular pH or have other physiological effects. Too much DAC expression could also overtax the Sec system (responsible for placing integral membrane proteins into the cell membrane) and inhibit the translocation of other membrane proteins necessary for cellular function (17).

With respect to the *T. ruber* DAC, it is not clear whether expression was successful. Expression controlled by a native promoter-rescued CO_2-sensitive *E. coli* strain, and growth was robust when controlled by a T7 promoter. However, intracellular DIC concentrations were not measurably higher when this complex was expressed, and presence of the DAC could not be confirmed via mass spectrometry. It is possible that this complex was expressed too weakly to provide a signal for the proteomic analysis and DIC measurement, while still providing the small amounts of DIC uptake necessary to sustain growth by *E. coli*. Another factor could be related to the host organism's habitat; *T. ruber* was the only hyperthermophile in this study. It is likely that the temperatures used for expression (37°C) and measuring DIC accumulation (21°C) were not optimal for its activity. Intracellular DIC concentrations were not elevated when uptake experiments were repeated at 37°C (data not shown). The DAC from this organism may require much higher temperature for optimal function.

For DACs composed of two or three subunits, all subunits are needed for DIC accumulation, which is consistent with prior studies of 2-subunit DACs (8, 14, 16). The M

TABLE 5 Effect of CCCP and its solvent (DMSO) on the intracellular pH and ATP content of *E. coli*

Addition	pH[a]	% ATP vs control[a]
None	7.58 ± 0.13	100 ± 4
0.1% DMSO	7.66 ± 0.18	40.3 ± 2.0[b]
0.1 mM CCCP + 0.1% DMSO	6.92 ± 0.12[b]	3.4 ± 0.4[b]

[a]Values are means and standard deviations from 8 (pH) and 4 (ATP) measurements.
[b]Statistically distinguishable ($P < 0.001$; Bonferroni *post hoc* test) from the value for incubations with no additions.

TABLE 6 Gene abundances gathered from metagenome data

pH category	pH range	No. of metagenomes	Total no. of genes	No. of DAC (COG3002)	No. of Sbt (COG3329)	COG ratio, DAC/Sbt[a]	No. of DAC (Pfam10070)	No. of Sbt (Pfam05982)	Pfam ratio, DAC/Sbt[b]
Acidic	0.83–5.4	91	2.7×10^7	864	180	4.8	701	159	4.4
Alkaline	8.5–10	74	3.4×10^7	1,439	3,329	0.43	1,153	3,266	0.35
Very alkaline	11–14	23	3.73×10^6	142	996	0.14	138	976	0.14

[a]Calculated as no. of DAC (COG3002)/no. of Sbt (COG3329).
[b]Calculated as no. of DAC (Pfam10070)/no. of Sbt (Pfam05982).

subunit, though predicted to have multiple membrane-spanning alpha helices, cannot act as a permease by itself. As demonstrated with this study, 3-subunit DACs also require the presence of the T subunit for activity; expression of the M subunit and the C subunit without the T subunit from *Acidithiobacillus thiooxidans*, *H. neapolitanus*, and *Sulfurovum* sp. strain AR also failed to accumulate intracellular DIC. The T subunits for these three complexes all have predicted transmembrane helices, suggesting that they may be involved in transport of DIC across the membrane, if DACs act as DIC transporters. Alternatively, the T subunit may play a regulatory role like that of the Sbt transporter regulatory subunit, SbtB. The SbtB subunit acts as like PII regulatory protein, modulating HCO_3^- transport by adenylylation (9, 18).

DIC accumulation by DACs appears to be universally linked to the proton motive force, as five structurally diverse DACs have now been shown to be sensitive to CCCP (15, 16, 19; this study). One possible mechanism to connect DIC accumulation to the proton motive force would be for DIC accumulation to rely on proton import, as has been suggested previously (16). The M subunit belongs to a protein family that includes subunits from other complexes that act to transport protons. One complex with subunits homologous to M subunits is the NADH dehydrogenase complex (including NuoL, ND5, and NdhF), which oxidizes NADH while contributing to cellular proton potential via proton expulsion. The other complexes with subunits homologous to M subunits are Mrp (multiple resistance and pH)-type Na^+/H^+ antiporters (14).

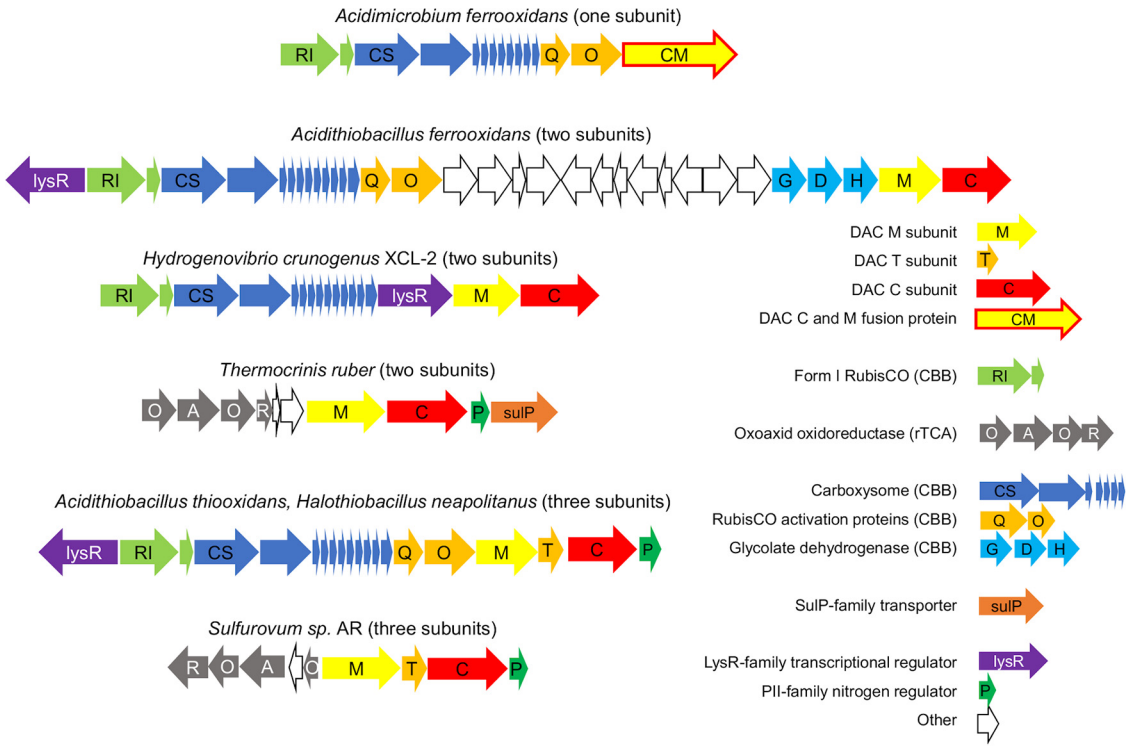

FIG 7 Chromosomal colocation of genes encoding DACs with those encoding enzymes from the CBB and rCAC pathways for autotrophic CO_2 fixation.

These antiporters contain either six or seven transmembrane subunits that function to maintain intracellular pH and sodium homeostasis (20).

Two possible models of DAC function are consistent with the data presented here (Fig. 1). In one model, proton translocation is coupled to conversion of intracellular CO_2 to HCO_3^- (16). This model is similar to the action of the modified NADH dehydrogenases used by some *Cyanobacteria*, which act as unidirectional carbonic anhydrases, converting intracellular CO_2 to HCO_3^- to prevent it from leaking from the cell (13, 21). Consistent with this proposed activity, C subunits from DAC are homologous to β-type carbonic anhydrases (16). Interestingly, the sequences of the genes encoding these systems in *Cyanobacteria* do not provide evidence for homology with those encoding DAC, suggesting independent evolutionary origins for the two types of complexes, which is consistent with other differences in mechanism. The systems in *Cyanobacteria* couple CO_2 hydration to redox reactions, while the amino acid sequences of DAC subunits do not suggest a link to such reactions (16). The other possible model for DAC function is that it acts as a CO_2:H^+ symporter (Fig. 1). In this case, CO_2 and H^+ would both be transported across the cell membrane. Upon arrival in the cytoplasm, the CO_2 could be converted to HCO_3^- by vectoral carbonic anhydrase activity by the DAC, as described above. Both models of DAC activity would result in elevated intracellular DIC concentrations, so it is not possible to determine which model is more likely to be correct at this point.

If DACs act as DIC transporters, it is interesting that they use CO_2 as a substrate, and not HCO_3^-. All the DIC transporters found in *Bacteria* thus far (SbtA, SulP, and BCT1) transport HCO_3^-. Metagenomics data also supports DAC using CO_2 as a substrate. The increased frequency of DAC over Sbt genes in metagenomes from more acidic environments would be beneficial, since CO_2 is more readily available than HCO_3^- at lower pH. Transporting CO_2 would make DAC unique among DIC transporters currently characterized in *Bacteria*. Though it seems counterintuitive that a CO_2 transporter would facilitate CO_2 entry into a cell, since CO_2 can diffuse through cell membranes, CO_2 entry and capture when DACs are expressed is much higher than in their absence (Fig. 5).

Consistency in DIC accumulation by these seven DACs, as well as those studied previously, strongly suggests that other members of this family throughout the tree of life likely also act to elevate intracellular DIC concentrations for the myriad of autotrophic and heterotrophic organisms in which they are found. The relative ease of heterologous expression of DACs from multiple phyla makes them an attractive tool for enhancing the activity of engineered organisms that convert CO_2 to industrial precursor compounds. In addition, the DACs studied here operate in organisms inhabiting habitats with acidic to basic pH values and low to high temperatures, which suggests that they could operate well in industrial contexts with similarly challenging environmental conditions. Though DACs were initially detected in a deep-sea sulfur chemolithoautotroph (14), their activity on DIC, a metabolite of near-universal importance to life, has implications for the ecophysiology of CO_2 fixation in many habitats, as well as carbon-neutral industry.

MATERIALS AND METHODS

Construction of plasmids for expressing DACs. Genes encoding DACs from seven taxonomically diverse organisms were inserted into three vectors, each with a different promoter: native (pENTR) (Thermo Fisher Scientific), T7 (pET28) (EMD Biosciences) and $araB_p$, the promoter from the *araBAD* operon (pBAD202) (Invitrogen, Inc.).

These constructs were synthesized by the Department of Energy Joint Genome Institute. First, sequences of genes encoding the presumed subunits of the complexes were optimized for expression in *E. coli* via BOOST (22). Then, genes encoding the 1, 2, and 3 presumed subunits of each complex were synthesized as linear DNA fragments (Twist Biosciences Inc., CA) and Gibson assembled using the NEBuilder HiFi DNA assembly master mix (New England Biolabs) with vectors carrying one of three different promoters: native (presumably weak in *E. coli*), pBAD (tightly regulated), or attenuated T7 (strong and regulated).

For constructs with native promoters, bacterial promoters were predicted from the genome sequences of the native organisms using BProm (23). DAC genes from *Am. ferrooxidans*, *Acidithiobacillus ferrooxidans*, *At. thiooxidans*, *H. neapolitanus*, *H. crunogenus*, and *T. ruber* appear to be distal to the beginning of

TABLE 7 Regions of host organism genomes predicted to encode native promoters for the operons in which the DAC genes were colocated, which were cloned into pENTR

Host organism	Region with promoter
Am. ferrooxidans	300-nucleotide intergenic region upstream from *cbbL* (IMG gene ID 644951266)
At. thiooxidans	200-nucleotide intergenic region upstream from *cbbL* (IMG gene ID 2838919118)
H. neapolitanus	200-nucleotide intergenic region upstream from *cbbL* (IMG gene ID 646383307)
Sulfurovum sp. AR	200-nucleotide intergenic region upstream from oxoacid oxidoreductase delta subunit (IMG gene ID 2620607603)
H. crunogenus	200-nucleotide intergenic region upstream from *cbbL* (IMG gene ID 637785558)
T. ruber	200-nucleotide intergenic region upstream from gene encoding leucyl-tRNA synthetase (IMG gene ID 2512918840)

an operon and do not have promoters predicted upstream. For each of these genes, a 200- to 300-nucleotide extension was added to the 5′ end of the sequence encoding the DAC (Table 7). This extension contained the promoter 5′ to the apparent operon that includes the DAC. Synthesized DNA was cloned into pENTR (Thermo Fisher Scientific).

For constructs in which expression was regulated via $araB_p$ in pBAD202 (Invitrogen, Inc.), sequences were optimized, and DNA was synthesized as described above and cloned into pBAD202 digested with NcoI and PmeI to remove all fusion domains so that the expressed proteins would have native amino and carboxy termini. For constructs regulated via T7 promoter, DNA was cloned into pET28b vector (EMD Biosciences) digested with NcoI and XhoI.

Constructs were also created to determine which of the presumed subunits of the complexes were responsible and/or necessary for DIC accumulation. For all DACs except the one from *Am. ferrooxidans*, in which M and C subunits are fused into a single protein (MC), constructs were created that carried only the gene encoding the M subunit. For DACs predicted to include a T subunit, constructs were created in which this subunit was absent. Genes were either synthesized as described above or amplified from the initial construct via PCR, and Gibson chewback cloned into pBAD202 or pET28b at the cloning sites described above. All constructs were sequence verified by PacBio sequencing (Pacific Biosciences, Inc., CA), and plasmids were introduced into *E. coli* TOP10 (Thermo Fisher Scientific).

Construction of *E. coli* host strain for expressing DACs. An *E. coli* strain was created to test the ability of the DAC to elevate intracellular DIC concentrations (described in the supplemental material). Like other heterotrophs, *E. coli* requires HCO_3^- for essential biological processes and thus requires carbonic anhydrase (CA) to convert cytoplasmic CO_2 to HCO_3^- (24). *E. coli* expressed two isoforms of CA: YadF, which is expressed when cells are growing slowly, and CynT, which is expressed when cells are using cyanate as a nitrogen source (25). *E. coli* EDCM636, in which *yadF* had been deleted, had previously been used to study DIC transporters (25) but was prone to pseudoreversion via expression of *cynT*. *E. coli* in which both CA genes are deleted is more stable and has been successfully used to express DACs from *H. neapolitanus*, *V. cholerae*, and *B. anthracis* (16), but this strain lacks a gene encoding T7 RNA polymerase. To avoid pseudoreversions, as well as to facilitate gene expression from multiple promoters, both CA genes were deleted from *E. coli* Lemo21(DE3). This strain of *E. coli* carries pLysS, encoding T7 RNA polymerase but also encodes a T7 lysozyme to provide the option of attenuating expression by T7 RNA polymerase (26).

Primers used for overlap extension PCR and PCR conditions are listed in Tables 8 and 9. Overlap extension PCR products, in which the target genes (*yadF* and *cynT*) were deleted, were cloned into suicide vector pLD55 (27). Selection of single and double crossovers, resulting in loss of *cynT* and *yadF*, was undertaken as described in reference 27. A detailed description of the steps to create *E. coli* Lemo21 (DE3) Δ*yadF* Δ*cynT* is provided in the supplemental material.

Chemically competent *E. coli* Lemo21(DE3) Δ*yadF* Δ*cynT*. *E. coli* Lemo21(DE3) Δ*yadF* Δ*cynT* was made chemically competent using the $CaCl_2$ method (28). Preparation of competent cells was as described in reference 29 with the following modifications. Bacteria were pelleted from 200 ml LB supplemented with chloramphenicol (30 mg/liter) under a 5% CO_2 headspace. The culture was resuspended in 12 ml 0.1 mM $CaCl_2$ and then incubated on ice for 30 min. Cells were harvested via centrifugation (1,500 × *g* for 10 min at 20°C). The pellets were resuspended in 3.2 ml 1 M $CaCl_2$ with 15% glycerol (vol/vol) and stored at −80°C.

Expressing DAC genes in *E. coli* Lemo21(DE3) Δ*yadF* Δ*cynT*. Plasmids carrying DAC genes (see "Construction of plasmids for expressing DACs," above) were purified from *E. coli* Top10 using the QIAprep spin minikit (Qiagen) and introduced into the chemically competent *E. coli* Lemo21(DE3) Δ*yadF* Δ*cynT* cells described above. Transformations were conducted as described in reference 29 with the following modifications. Mixed DNA and competent cells were stored on ice for 15 min. A recovery period of 1 h at 37°C was used. Each reaction mixture was plated on solid LA supplemented with the appropriate antibiotic (depending on the vector; 25 mg/liter kanamycin for pENTR vectors, 25 mg/liter kanamycin for pET28 vectors, and 30 mg/liter apramycin for pBAD202 vectors) and incubated for 24 h at 30°C in a high-CO_2 incubation chamber. PCR assays (Tables 8 and 9) were used to confirm that the pLD55 plasmids containing the C and M subunits (as appropriate) were successfully carried by the *E. coli* Lemo21 (DE3) Δ*yadF* Δ*cynT* cells after transformation.

Cells were grown in 20-ml liquid cultures using LB with 25 mg/liter kanamycin for pET28 vectors, and 30 mg/liter apramycin for pBAD202 vectors. For DACs whose expression was driven by the T7 promoter, IPTG (1 mM) was added to growth media to induce expression and rhamnose (2 mM) to repress expression. Media for DACs whose expression was driven by $araB_p$ were supplemented with 6 mM

TABLE 8 PCR primer sequences

Purpose and organism	Primer sequence (5′→3′)	
	Forward	Reverse
Amplifying region upstream of *yadF*	GAG AAC TAG TTT GCG TTT TCC CCA TAG ATC GAG TTG TTT AAG ATA T	GCA TCC GGC ATG GCA TTT GGA GGT TAA CGA CCT GTA ACC
Amplifying region downstream of *yadF*	AAA TGC CAT GCC GGA TGC AAC A	GAG AAC TAG TTG AGC GTT ACA AAG ACA GTG GC
Amplifying region upstream of *cynT*	GAG AAC TAG TTT CTC CTG CGA CAT TTC CTG TAG CTG	TGG AAC TCC TGA TGG TTT AAA AAT AAG GCG TTA ACC TCT GTC TGT CTC TG
Amplifying region downstream of *cynT*	CCT TAT TTT TAA ACC ATC AGG AGT TCC A	GAG AAC TA TCA GAA CGG TTT GTT CGG CAG ATA TTT ACC
Purification PCR, *yadF*	GAG AAC TAG TTT GCG TTT TCC CCA TAG ATC GAG TTG TTT AAG ATA T	GAG AAC TAG TTG AGC GTT ACA AAG ACA GTG GC
Purification PCR, *cynT*	GAG AAC TAG TTT CTC CTG CGA CAT TTC CTG TAG CTG	GAG AAC TA TCA GAA CGG TTT GTT CGG CAG ATA TTT ACC
Verifying presence of OE PCR product in pLD55	ATG ACC ATG ATT ACG CCA AGC	CCC CGA TTT AGA GCT TGA CG
Verifying presence of plasmids carrying complete set of DAC genes		
Am. ferrooxidans	TTC GCA TAG CGG AAG TGT ATT	GAA GGC ACC CGT GTA GAT G
At. ferrooxidans	CGA CGA TCC AGA AGC TCA ATA C	AAA GTA CGC CGC GCA ATA
At. thiooxidans	CGG GCG TTG GCA TTA TTT AC	GGG TTT CGT CGT CTT GAT CT
H. crunogenus	GAT GGT TGT GGG CTT GAT TTG	TCG CCA ACC ACT CAT GAT AAA
H. neapolitanus	GGC GCA TAG CTC CAT CTT AT	GAG TCA GTT CGC GGG TAA TC
Sulfurovum sp. strain AR	TTG ATC ACC CTT GCA CTC TAT C	AAT CCT GCC CAA CCA TGA A
T. ruber	TGC CTA TCT ACT CCC TTC TGT	GGG TTA TGT ATC CCT CCC AAA G
Verifying presence of plasmids encoding incomplete set of DAC genes		
At. ferrooxidans (M only)	ATGATTACATCCTCTCTTCTTATGTTGGT	GTA CGG CGA TAC TGT ACA AAC C
At. thiooxidans (M only)	ATG GGT AAT TGG GCA ATT GCA	AAC CGT GGG CGA TCA G
At. thiooxidans (no T)	ATG GGT AAT TGG GCA ATT GCA	AAC CGT GGG CGA TCA G
H. crunogenus (M only)	ATG AAT ATG CAA TGG GTA GGG G	TTA AGA AGG CAT AAG CTT TGT AAC AAG AG
H. neapolitanus (M only)	ATG ATG AAC CTG CAA TGG TTA ATT CC	GAC CAT GCG CAA TGA GAT GG
H. neapolitanus (no T)	GGC GCA TAG CTC CAT CTT AT	GAG TCA GTT CGC GGG TAA TC
Sulfurovum sp. strain AR (M only)	ATG GAA AAG ATT ATA TTG CTC ATT CCA GC	CCA AGA AGA GTG TTG CTT TAA AGA CAC
Sulfurovum sp. strain AR (no T)	ATG GAA AAG ATT ATA TTG CTC ATT CCA GC	AAT CCT GCC CAA CCA TGA A
T. ruber (M only)	ATG GTT CTT GAA GCA ATC ATC GT	GGT CTT TTC TTG CCT CGT GT

TABLE 9 PCR conditions

Purpose	Temp [°C] (time [min])			No. of cycles
	Denaturing	Annealing	Extension	
Amplifying upstream regions	95 (1)	60 (6)	72 (2)	10
	95 (1)	60 (3)	72 (2)	20
Amplifying downstream regions	95 (1)	60 (1)	72 (2)	25
Overlap PCR	95 (1)	55 (1)	72 (1.5)	15
Purification PCR	95 (1)	60 (1)	72 (1.5)	30
Verifying presence of OE PCR product in pLD55	95 (1)	50 (1)	72 (1.5)	25
Verifying presence of DAC genes	95 (1)	50 (1)	72 (1)	25

arabinose. For *E. coli* expressing the DAC from *Sulfurovum* sp. strain AR, growth yields were higher when arabinose concentrations were dropped to 1.2 mM (Fig. S4), presumably by lowering the expression of the DACs to diminish deleterious effects on the cells (17).

LC-MS/MS was used to confirm the expression of DAC genes in *E. coli* Lemo21(DE3) Δ*yadF* Δ*cynT* as described in reference 14 with the following modifications. A 120-min gradient was used for peptide separation by a C_{18} reversed-phase high-performance liquid chromatography column prior to analysis on a Q Exactive Plus instrument (Thermo Fisher Scientific), and raw data files were processed in MaxQuant, version 1.6.17.0.

Growth of *E. coli* constructs expressing DACs. As an initial screen to determine whether expression of DACs stimulated growth under low DIC conditions, strains were propagated on solid lysogeny medium with low CO_2 (ambient air, 0.04% CO_2) and high CO_2 (5% CO_2). Cells were grown under conditions that either induced or repressed gene expression, as described above. Once growth was confirmed on solid medium, cells were cultivated in liquid medium. Cells were cultivated in 20 ml liquid lysogeny broth in 250-ml flasks, under ambient air or a 5% CO_2–95% air headspace at 100 rpm and 37°C, and growth was monitored via optical density at 600 nm (OD_{600}) to measure the effects of DIC, inducer (1 mM IPTG or 6 mM arabinose; see above), or repressor (2 mM rhamnose or 0.2% glucose; see above).

Intracellular DIC concentrations in *E. coli* expressing DACs. Cultures expressing each of the seven DACs were grown in LB under a 5% CO_2 atmosphere with the appropriate antibiotic and inducers. Cells were harvested by centrifugation (10,000 × *g*, 5 min, 4°C), washed once in fresh LB, resuspended to an OD_{600} of 5, and kept on ice for immediate quantification of DIC accumulation by silicone oil centrifugation as described in reference 8, with the following modifications. Cell suspensions were mixed into to a modified assay buffer (LB, 50 mM Na-HEPES [pH 8], 0.25 mM $NaH^{14}CO_3^-$ [2 mCi/mM]). This mixture was then carefully pipetted into microcentrifuge tubes with silicone oil overlying a killing solution and centrifuged, and the pellet was assayed via scintillation counting in order to quantify intracellular [^{14}C]DIC (8).

DAC substrate: HCO_3^- or CO_2. DACs from three bacteria, *Am. ferrooxidans*, *H. crunogenus*, and *Sulfurovum* sp. strain AR, were chosen for further investigation. These three DACs included all three subunit compositions (1 subunit, 2 subunit, and 3 subunit), three phyla (*Actinobacteria*, *Proteobacteria*, and *Campylobacterota*), and a broad range of habitat pH values (acidic to alkaline). These DACs were tested to determine if they were active with CO_2 versus HCO_3^- by performing isotopic disequilibrium experiments as described in reference 30. This technique relies on the slowness of interconversion of CO_2 and HCO_3^- in the absence of CA (30). To prepare for isotopic disequilibrium experiments, a solution of $^{14}CO_2$ was prepared by adding [^{14}C]DIC stock solution to 1 mM H_3PO_4 in a sealed serum vial and allowing it to equilibrate for 5 min. To measure CO_2 uptake, cells were suspended in 200 μl of 50 mM HEPES-buffered LB (pH 8) and layered on top of silicone oil and killing solution as described in reference 30. Ten microliters of $^{14}CO_2$ solution was added, and after a 20-s incubation, cells were centrifuged into the killing solution and processed as described in reference 30. To measure $H^{14}CO_3^-$ uptake, the incubation solution was supplemented with bovine carbonic anhydrase (0.1 mg/ml), which instantaneously converts ~99% of the CO_2 to HCO_3^- and CO_3^{2-}, assuming a pKa for carbonic acid of 6.1 and an incubation pH of 8. Ten microliters of $^{14}CO_2$ solution was added and presumably instantaneously converted to HCO_3^-, and cells were incubated and processed as described above.

Use of proton potential for DIC accumulation. To investigate the mechanism of DIC uptake, the proton potential was collapsed using the protonophore carbonyl cyanide *m*-chlorophenylhydrazone (CCCP) as described in reference 14. CCCP solutions were prepared in DMSO (100 mM). Cells were incubated for 2 min in the presence of 0.1% DMSO (solvent control) or 0.1 mM CCCP dissolved in DMSO before intracellular DIC concentrations were measured as described above. To verify that the CCCP affected proton potential in these cells, the effect of this inhibitor was also measured on intracellular ATP with an ATP bioluminescence assay kit (Sigma). Effects on the proton potential were also verified by measuring intracellular pH using [^{14}C]methylamine, an ammonia derivative that accumulates in the cytoplasm to a level proportional to pH, as described in reference 30.

Relative abundance of genes encoding DACs and Sbt transporters in metagenomes from alkaline and acidic environments. To determine whether the pH of the habitat influences the abundance of DIC accumulation mechanisms acting on CO_2 (DACs) versus HCO_3^- (Sbt transporters), metagenomes for which habitat pH data were available were collected from the Integrated Microbial Genomes and Microbiomes database (https://img.jgi.doe.gov/) (31). These metagenomes were searched for genes

belonging to Pfam 10070 and COG 3002 (encoding DACs) and Pfam 05982 and COG 3329 (encoding Sbt transporters). Data were divided into three groups based on habitat pH: acidic (pH $<$ 5.5), alkaline (pH = 8.5 to 10), and very alkaline (pH $>$ 10). Relative abundance was calculated from the DAC/Sbt ratio.

Data availability. Nucleotide sequences of inserts including genes encoding DAC subunits and native promoters are available at GenBank (accession numbers MZ935230 to MZ935251).

SUPPLEMENTAL MATERIAL

Supplemental material is available online only.

SUPPLEMENTAL FILE 1, PDF file, 0.3 MB.

ACKNOWLEDGMENTS

The work conducted by the U.S. Department of Energy Joint Genome Institute, a DOE Office of Science User Facility, is supported under contract DE-AC02-05CH11231. We thank NSF (NSF- MCB-1952676 to K.M.S.), the University of South Florida, and the Porter Family Foundation for their financial support for this project.

We are grateful to the anonymous reviewers for their helpful suggestions.

We declare no conflict of interest.

REFERENCES

1. Sievert SM, Vetriani C. 2012. Chemoautotrophy at deep-sea vents past, present, and future. Oceanograpy 25:218–233. https://doi.org/10.5670/oceanog.2012.21.
2. Colman DR, Lindsay MR, Amenabar MJ, Boyd ES. 2019. The intersection of geology, geochemistry, and microbiology in continental hydrothermal systems. Astrobiology 19:1505–1522. https://doi.org/10.1089/ast.2018.2016.
3. Lenk S, Arnds J, Zerjatke K, Musat N, Amann R, Mussmann M. 2011. Novel groups of *Gammaproteobacteria* catalyse sulfur oxidation and carbon fixation in a coastal, intertidal sediment. Environ Microbiol 13:758–774. https://doi.org/10.1111/j.1462-2920.2010.02380.x.
4. Hedrich S, Schippers A. 2021. Distribution of acidophilic microorganisms in natural and man-made acidic environments. Curr Issues Mol Biol 40:25–47. https://doi.org/10.21775/cimb.040.025.
5. Johnson KS, Childress JJ, Beehler CL. 1988. Short term temperature variability in the Rose Garden hydrothermal vent field. Deep Sea Res 35:1711–1722. https://doi.org/10.1016/0198-0149(88)90045-3.
6. Goffredi SK, Childress JJ, Desaulniers NT, Lee RW, Lallier FH, Hammond D. 1997. Inorganic carbon acquisition by the hydrothermal vent tubeworm *Riftia pachyptila* depends upon high external P-CO_2 and upon proton-equivalent ion transport by the worm. J Exp Biol 200:883–896. https://doi.org/10.1242/jeb.200.5.883.
7. Price GD. 2011. Inorganic carbon transporters of the cyanobacterial CO_2 concentrating mechanism. Photosynth Res 109:47–57. https://doi.org/10.1007/s11120-010-9608-y.
8. Scott KM, Leonard JM, Boden R, Chaput D, Dennison C, Haller E, Harmer TL, Anderson A, Arnold T, Budenstein S, Brown R, Brand J, Byers J, Calarco J, Campbell T, Carter E, Chase M, Cole M, Dwyer D, Grasham J, Hanni C, Hazle A, Johnson C, Johnson R, Kirby B, Lewis K, Neumann B, Nguyen T, Nino Charari J, Morakinyo O, Olsson B, Roundtree S, Skjerve E, Ubaldini A, Whittaker R. 2019. Diversity in CO_2 concentrating mechanisms among chemolithoautotrophs from the genera *Hydrogenovibrio*, *Thiomicrorhabdus*, and *Thiomicrospira*, ubiquitous in sulfidic habitats worldwide. Appl Environ Microbiol 85:e02096-18. https://doi.org/10.1128/AEM.02096-18.
9. Scott KM, Harmer TL, Gemmell BJ, Kramer AM, Sutter M, Kerfeld CA, Barber KS, Bari S, Boling JW, Campbell CP, Gallard-Gongora JF, Jackson JK, Lobos A, Mounger JM, Radulovic PW, Sanson JM, Schmid S, Takieddine C, Warlick KF, Whittaker R. 2020. Ubiquity and functional uniformity in CO_2 concentrating mechanisms in multiple phyla of Bacteria is suggested by a diversity and prevalence of genes encoding candidate dissolved inorganic carbon transporters. FEMS Microbiol Lett 367:fnaa106. https://doi.org/10.1093/femsle/fnaa106.
10. Omata T, Takahashi Y, Yamaguchi O, Nishimura T. 2002. Structure, function, and regulation of the cyanobacterial high-affinity bicarbonate transporter, BCT1. Funct Plant Biol 29:151–159. https://doi.org/10.1071/PP01215.
11. Price G, Woodger F, Badger M, Howitt S, Tucker L. 2004. Identification of a SulP-type bicarbonate transporter in marine cyanobacteria. Proc Natl Acad Sci U S A 101:18228–18233. https://doi.org/10.1073/pnas.0405211101.
12. Shibata M, Katoh H, Sonoda M, Ohkawa H, Shimoyama M, Fukuzawa H, Kaplan A, Ogawa T. 2002. Genes essential to sodium-dependent bicarbonate transport in cyanobacteria. J Biol Chem 277:18658–18664. https://doi.org/10.1074/jbc.M112468200.
13. Han X, Sun N, Xu M, Mi H. 2017. Co-ordination of NDH and Cup proteins in CO_2 uptake in cyanobacterium *Synechocystis* sp. PCC 6803. J Exp Bot 68:3869–3877. https://doi.org/10.1093/jxb/erx129.
14. Mangiapia M, MicrobialPhysiology U, Brown T-RW, Chaput D, Haller E, Harmer TL, Hashemy Z, Keeley R, Leonard J, Mancera P, Nicholson D, Stevens S, Wanjugi P, Zabinski T, Pan C, Scott KM, USF MCB4404L. 2017. Proteomic and mutant analysis of the CO_2 concentrating mechanism of hydrothermal vent chemolithoautotroph *Thiomicrospira crunogena*. J Bacteriol 199:e00871-16. https://doi.org/10.1128/JB.00871-16.
15. Fan SH, Ebner P, Reichert S, Hertlein T, Zabel S, Lankapalli AK, Nieselt K, Ohlsen K, Gotz F. 2019. MpsAB is important for *Staphylococcus aureus* virulence and growth at atmospheric CO_2 levels. Nat Commun 10:3627. https://doi.org/10.1038/s41467-019-11547-5.
16. Desmarais JJ, Flamholz AI, Blikstad C, Dugan EJ, Laughlin TG, Oltrogge LM, Chen AW, Wetmore K, Diamond S, Wang JY, Savage DF. 2019. DABs are inorganic carbon pumps found throughout prokaryotic phyla. Nat Microbiol 4:2204–2215. https://doi.org/10.1038/s41564-019-0520-8.
17. Wagner S, Klepsch MM, Schlegel S, Appel A, Draheim R, Tarry M, Högbom M, van Wijk KJ, Slotboom DJ, Persson JO, de Gier J-W. 2008. Tuning *Escherichia coli* for membrane protein overexpression. Proc Natl Acad Sci U S A 105:14371–14376. https://doi.org/10.1073/pnas.0804090105.
18. Kaczmarski JA, Hong N-S, Mukherjee B, Wey LT, Rourke L, Förster B, Peat TS, Price GD, Jackson CJ. 2019. Structural basis for the allosteric regulation of the SbtA bicarbonate transporter by the PII-like protein, SbtB, from *Cyanobium* sp. PCC7001. Biochemistry 58:5030–5039. https://doi.org/10.1021/acs.biochem.9b00880.
19. Menning KJ, Menon BB, Fox G, Scott U, USF MCB4404L 2012. 2016. Dissolved inorganic carbon uptake in *Thiomicrospira crunogena* XCL-2 is Dp- and ATP-sensitive and enhances RubisCO-mediated carbon fixation. Arch Microbiol 198:149–159. https://doi.org/10.1007/s00203-015-1172-6.
20. Ito M, Morino M, Krulwich TA. 2017. Mrp antiporters have important roles in diverse Bacteria and Archaea. Front Microbiol 8:2325. https://doi.org/10.3389/fmicb.2017.02325.
21. Gaudana SB, Zarzycki J, Moparthi VK, Kerfeld CA. 2015. Bioinformatic analysis of the distribution of inorganic carbon transporters and prospective targets for bioengineering to increase C_i uptake by cyanobacteria. Photosynth Res 126:99–109. https://doi.org/10.1007/s11120-014-0059-8.
22. Oberortner E, Cheng J-F, Hillson NJ, Deutsch S. 2017. Streamlining the design-to-build transition with build-optimization software tools. ACS Synth Biol 6:485–496. https://doi.org/10.1021/acssynbio.6b00200.
23. Umarov RK, Solovyev VV. 2017. Recognition of prokaryotic and eukaryotic promoters using convolutional deep learning neural networks. PLoS One 12:e0171410. https://doi.org/10.1371/journal.pone.0171410.
24. Sutter M, Roberts EW, Gonzalez RC, Bates C, Dawoud S, Landry K, Cannon GC, Heinhorst S, Kerfeld CA. 2015. Structural characterization of a newly identified component of alpha-carboxysomes: the AAA plus domain protein CsoCbbQ. Sci Rep 5:16243. https://doi.org/10.1038/srep16243.

25. Merlin C, Masters M, McAteer S, Coulson A. 2003. Why is carbonic anhydrase essential to *Escherichia coli*? J Bacteriol 185:6415–6424. https://doi.org/10.1128/JB.185.21.6415-6424.2003.
26. Schlegel S, Löfblom J, Lee C, Hjelm A, Klepsch M, Strous M, Drew D, Slotboom DJ, de Gier J-W. 2012. Optimizing membrane protein overexpression in the *Escherichia coli* strain Lemo21(DE3). J Mol Biol 423:648–659. https://doi.org/10.1016/j.jmb.2012.07.019.
27. Metcalf WM, Jiang W, Daniels LL, Kim S, Haldimann A, Wanner BL. 1996. Conditionally replicative and conjugative plasmids carrying *lacZa* for cloning, mutagenesis, and allele replacement in bacteria. Plasmid 35:1–13. https://doi.org/10.1006/plas.1996.0001.
28. Chan WT, Verma CS, Lane DP, Gan SK. 2013. A comparison and optimization of methods and factors affecting the transformation of *Escherichia coli*. Biosci Rep 33:e00086. https://doi.org/10.1042/BSR20130098.
29. Sambrook J, Russell DW. 2001. Molecular cloning: a laboratory manual. Cold Spring Harbor Laboratory Press, Cold Spring Harbor, NY.
30. Dobrinski KP, Longo DL, Scott KM. 2005. A hydrothermal vent chemolithoautotroph with a carbon concentrating mechanism. J Bacteriol 187:5761–5766. https://doi.org/10.1128/JB.187.16.5761-5766.2005.
31. Chen IA, Chu K, Palaniappan K, Pillay M, Ratner A, Huang J, Huntemann M, Varghese N, White JR, Seshadri R, Smirnova T, Kirton E, Jungbluth SP, Woyke T, Eloe-Fadrosh EA, Ivanova NN, Kyrpides NC. 2019. IMG/M v.5.0: an integrated data management and comparative analysis system for microbial genomes and microbiomes. Nucleic Acids Res 47:D666–D677. https://doi.org/10.1093/nar/gky901.
32. Krogh A, Larsson B, von Heijne G, Sonnhammer EL. 2001. Predicting transmembrane protein topology with a hidden Markov model: application to complete genomes. J Mol Biol 305:567–580. https://doi.org/10.1006/jmbi.2000.4315.
33. Clark DA, Norris PR. 1996. *Acidimicrobium ferrooxidans* gen. nov., sp. nov.: mixed-culture ferrous iron oxidation with *Sulfobacillus* species. Microbiology (Reading) 142:785–790. https://doi.org/10.1099/00221287-142-4-785.
34. Temple KL, Colmer AR. 1951. The autotrophic oxidation of iron by a new bacterium, *Thiobacillus ferrooxidans*. J Bacteriol 62:605–611. https://doi.org/10.1128/jb.62.5.605-611.1951.
35. Waksman SA, Joffe JS. 1922. Microörganisms concerned in the oxidation of sulfur in the soil: II. *Thiobacillus thiooxidans*, a new sulfur-oxidizing organism isolated from the soil. J Bacteriol 7:239–256. https://doi.org/10.1128/jb.7.2.239-256.1922.
36. Jannasch H, Wirsen C, Nelson D, Robertson L. 1985. *Thiomicrospira crunogena* sp. nov., a colorless, sulfur-oxidizing bacterium from a deep-sea hydrothermal vent. Int J Syst Bacteriol 35:422–424. https://doi.org/10.1099/00207713-35-4-422.
37. Parker CD, Genus V. 1957. *Thiobacillus* Beijerinck 1904, p 83–88. *In* Breed RS, Murray EGD, Smith NR (ed), Bergey's manual of determinative bacteriology. The Williams and Wilkins Co, Baltimore, MD.
38. Park BJ, Park SJ, Yoon DN, Schouten S, Sinninghe Damsté JS, Rhee SK. 2010. Cultivation of autotrophic ammonia-oxidizing archaea from marine sediments in coculture with sulfur-oxidizing bacteria. Appl Environ Microbiol 76:7575–7587. https://doi.org/10.1128/AEM.01478-10.
39. Huber R, Eder W, Heldwein S, Wanner G, Huber H, Rachel R, Stetter KO. 1998. *Thermocrinis ruber* gen. nov., sp. nov., a pink-filament-forming hyperthermophilic bacterium isolated from Yellowstone National Park. Appl Environ Microbiol 64:3576–3583. https://doi.org/10.1128/AEM.64.10.3576-3583.1998.